Chapter 20

Ionospheric Storms

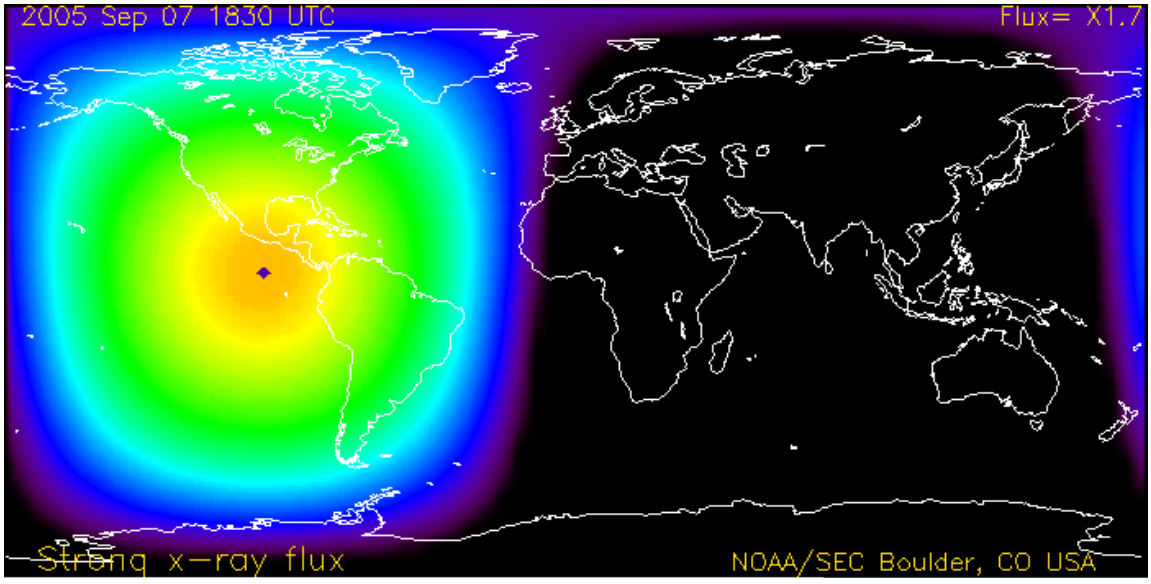

20 Ionospheric Storms

A sudden change in ionospheric conditions marks the onset of an ionospheric storm. A storm is caused by violent events occurring on the Sun and can last a few hours to several days or more.

During an ionospheric storm one of two things, or both, can occur.

- D region absorption of 160 thru 20 meter radio signals dramatically increases causing wide spread radio blackouts. Longer wavelength signals are affected the most.

- Critical frequencies suddenly drop adversely affecting 20 through 10 meter communications with shorter wavelength signals being affected the most.

Ionospheric storms are much different than the better known geomagnetic storms.

Geomagnetic storms cause significant dips and fluctuations in Earth's magnetic field as illustrated in Figure 1. A fluctuating magnetic field can seriously disrupt electrical power distribution grids causing millions of people to lose electrical power for several hours to several months. Geomagnetic storms also induce dangerous electric currents into long pipelines and railroad tracks, affect airline travel on routes over the polar regions, increase satellite drag accelerating satellite end of life , and affect many other aspects of our technological world.

The most severe geomagnetic storm on record occurred in 1859. The storm disrupted telegraph communications, caused telegraph operators to receive severe electrical shocks, and in some cases started fires. It is estimated that a storm of that magnitude occurring today would cause over $2 trillion in damage. For this reason, fleets of spacecraft are in orbit around the Earth and Sun continuously monitoring solar activity. These spacecraft provides us with an early warning system of impending geomagnetic storms, providing us time to put critical systems into a "safe mode".

The most severe geomagnetic storm experienced in recent decades occurred in March 1989. This storm was the result of a coronal mass ejected from the Sun on March 9 th. The storm was so intense that it knocked out the Hydro Quebec electric power distribution system causing over 6 million people to lose electricity.

The Disturbance Storm Time (Dst) index shown in Figure 1 measures the severity of a geomagnetic storm. The Dst index is zero on geomagnetic quiet days. An index of -50 or greater indicates a storm-level disturbance in the magnetic field. An index of -200 or deeper signifies a severe storm that can cause considerable damage and produce aurorae visible as far south as Washington D. C. Notice in Figure 1 that the Dst index spiked down -600 nT on the 13th of March! The current Dst index is available by clicking on Dst Index under the Current Conditions tab of the www.skywave-radio.org web site.

The chapter on Geomagnetic Storms provides a more detailed discussion of these storms.

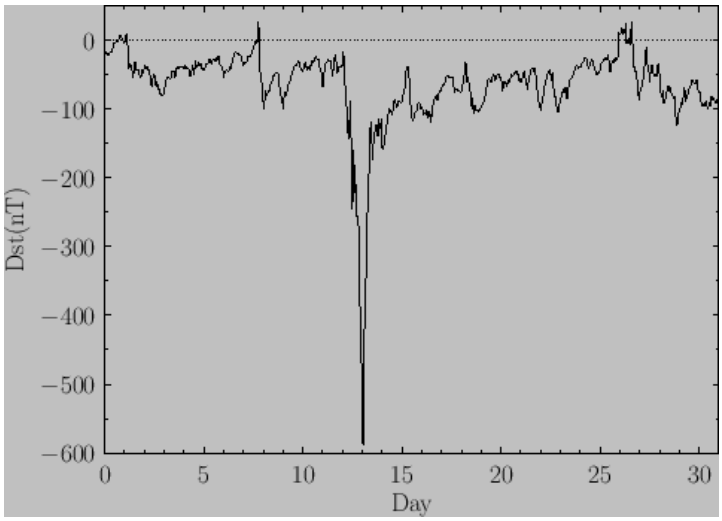

Figure 1 Dst index for the month of March 1989 (source: Farside.ph.utexas.edu)

In contrast, ionospheric storms cause perturbations in the ionosphere adversely affecting HF radio communications as illustrated in Figure 2.

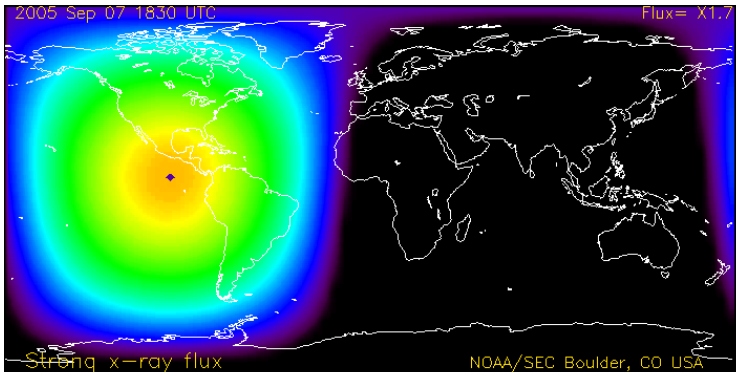

Figure 2 Ionospheric X-ray radiation storm (source: NOAA)

There are three types of ionospheric storms:

- X-ray radiation storms,
- High energy particle storms, and
- Solar wind storms.

Earth's polar cap region and auroral zones are the breeding grounds for high energy particle storms and solar wind storms. High energy particle storms remain localized in the polar regions causing Polar Cap Absorption (PCA) events that absorb transpolar HF radio signals. Long wavelength 160 through 20 meter signals are affected the most. Ionospheric solar wind storms originate in the auroral zone and drift down into the mid-latitudes carried along by thermospheric winds. Solar wind storms cause critical frequencies to drop by a factor of 2 or more seriously affecting mid-latitude and polar 20 through 10 meter communications for days. X-ray radiation storms immediately impact all daylight regions of the Earth, particularly those areas where the Sun is directly overhead as illustrated by the black diamond in Figure 2. X-ray radiation storms dramatically increase D region absorption preventing communications on 160 through 20 meters for the duration of the storm.

20.1 Solar Events Producing Ionospheric Storms

While ionospheric and geomagnetic storms are quite different, they are caused by the same violent solar events including:

- Collapsing Coronal Loops
- Solar Flares,
- Coronal Mass Ejections (CME),
- Coronal Holes, and
- Solar Winds

20.1.1 Collapsing Coronal Loops

Coronal loops are created by upwelling magnetic fields generated inside the Sun. The foot points of a coronal loop are anchored in the photosphere as shown in Figure 3. A coronal loop is huge compared to the Earth as dramatically illustrated by Figure 3. Coronal loops often form above sunspot groups in the active regions of the Sun magnetically connecting one region on the solar surface to another.

The plasma forming a coronal loop is extremely hot reaching temperatures of over 100,000 ^{o}K. The plasma consists primarily of ionized hydrogen, hydrogen being the primary constituent of the solar atmosphere as well of the Sun itself. At coronal loop temperatures all hydrogen atoms in the coronal loop plasma are fully ionized. That is, each atom is stripped of its one and only electron by the plasma's extreme temperature. The resulting hydrogen ion (a positively charged proton) cannot radiate light since it no longer has an electron capable of jumping between energy levels. Instead, a coronal loop's very hot plasma emits copious amounts of extreme ultraviolet and x-ray radiation. Coronal loop plasma also contains a few heavy ions such as iron. These ions still have a complement of electrons left after ionization that can emit light at discrete wavelengths. These emission lines are frequently used to determine the temperature and density of coronal loop plasma.

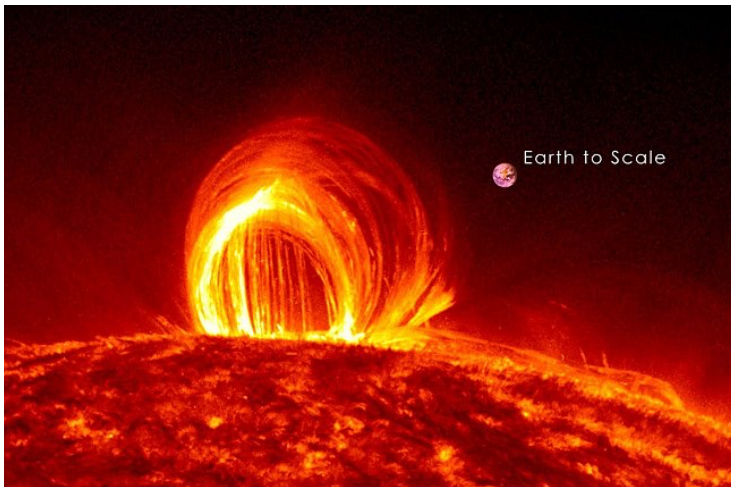

Figure 3 Coronal loop (source: NASA's Cosmos)

20.1.2 Solar Flares

A solar flare is a massive, sudden, explosive release of stored energy. Solar flares are huge. The solar flare shown in Figure 4 is larger than the Earth.

Figure 4 A solar flare (source: NASA)

A flare is often caused by the collapse of a coronal loop. The foot points anchoring a coronal loop to the photosphere move. If the foot points moved together, a coronal loop would rotate back and forth in a beautiful twirling dance. However, the foot points do not move together. Plasma flows in the

Sun's underlying convection zone in addition to the Sun's differential rotation cause the foot points to move independently, usually in different directions. This independent motion causes the coronal loop's magnetic field lines to become stretched out, twisted, and tangled into an hour-glass shape as illustrated in Figure 5.

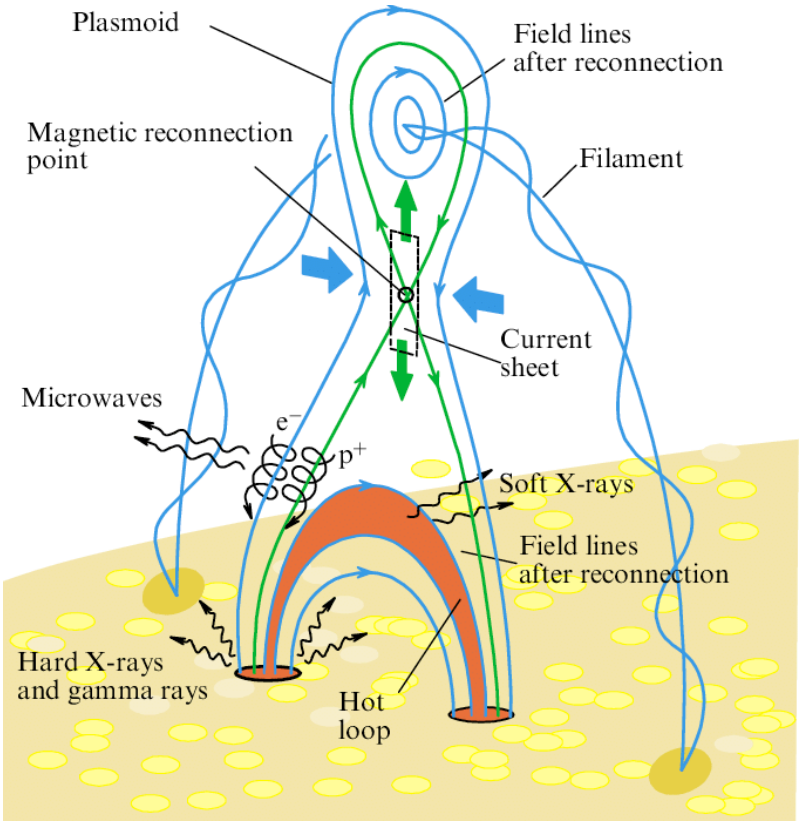

Figure 5 Formation of a solar flare (source: ResearchGate)

Outbound and returning magnetic field lines (the green lines in Figure 5) are squeezed closer and closer together forming the hour glass neck. Energy builds up rapidly in the neck region eventually becoming so great that outbound and returning magnetic field lines "short circuit" rupturing the coronal loop and initiating a solar flare.

Below the rupture, outbound and returning field lines reconnect into a much smaller hot magnetic loop anchored in the photosphere. Hot plasma consisting of energetic electrons plus hydrogen and helium nuclei stream down the reconnected field lines. These energetic particles are traveling at nearly the speed of light. Nuclear reactions are triggered as these particles crash into the upper chromosphere. The nuclear reactions release a massive amount of energy in the form of gamma

rays, x-rays, extreme ultra-violate light, visible light, and radio waves. The amount of energy typically released by a large flare is equivalent to millions of 100 – megaton hydrogen bombs exploding all at once. The x-ray and extreme ultra-violet radiation travels to Earth in 8 minutes triggering an ionospheric radiation storm.

Above the rupture, magnetic field lines also reconnect forming a plasmoid of hot electrons plus hydrogen and helium nuclei. These particles are accelerated to very high energy levels producing solar energetic particles (SEPs) and high-speed solar winds. The plasmoid rapidly expands into interplanetary space as a coronal mass ejection (CME). The SEPs trigger energetic particle storms in Earth's polar regions within 20 minutes to an hour following the flare, while high-speed solar winds produce ionospheric solar wind storms in 2 to 4 days.

20.1.3 Coronal Mass Ejections

A corona mass ejection (CME) is a huge eruption of coronal plasma, with its associated frozen-in magnetic field, that moves outward from the Sun into interplanetary space. CMEs vary widely in size, shape, and speed. Some look like loops, other like bubbles, and some are irregular in shape. Figure 6 is an example of a CME. To produce Figure 6 a disk was installed on the camera and positioned over the main part of the Sun, blocking the intense light from the photosphere, so that the corona mass ejection could be seen.

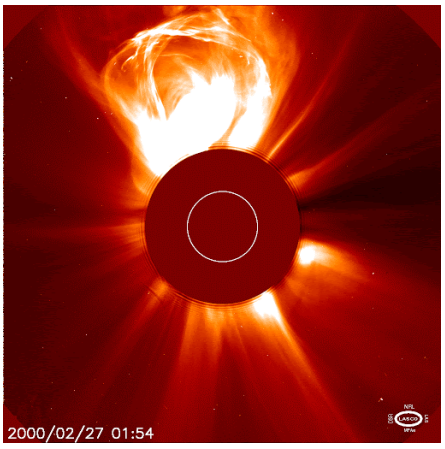

Figure 6 Coronal Mass Ejection (source: www.astronet.ru)

CMEs are often caused by the collapse of coronal loops as magnetic fields re-align and reconnect into lower energy states. A catastrophic collapse of coronal loops can trigger solar flares which also produce CMEs.

A CME can eject billions of tons of coronal material outward from the Sun at speeds typically ranging from 200 to 500 km/s. Note that 447 km/s is equal to 1 million per hour. Some energetic CMEs can reach speeds of 3,000 km/s or more. A shock wave is created when the CME travels

faster than the background solar wind. The shock wave often accelerates charged particles ahead of it which can trigger energetic particle storms as the CME impacts Earth. During solar maximum several CMEs of various sizes and shapes occur per day. At solar minimum one CME is typically observed every 5 days or so.

Most CMEs are ejected outward from the Sun into the solar system away from the Earth. However, a CME launched in Earth's direction can arrive in as little as 15-18 hours. Slower CMEs may take several days to arrive. A CME expands as it travels away from the Sun. A large CME can encompass nearly a quarter of the distance between the Sun and Earth by the time it reaches Earth.

20.1.4 Coronal Holes

Coronal holes are dark areas seen in the solar corona when viewed in EUV and soft X-ray light. They appear dark, like those shown in Figure 7, because they are cooler and less dense than the surrounding corona plasma.

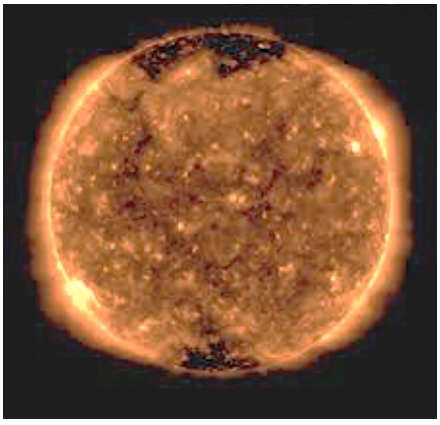

Figure 7 Large dark regions are coronal holes (source: NOAA www.swpc.noaa.gov/phenomena)

Coronal holes can develop at any time and any location on the Sun. However, they occur most often at the solar north and south poles. Some of these grow and expand into lower solar latitudes, while others spin off individual holes. Coronal holes can also develop at regions other than the solar poles. Coronal holes occur most often and last longer during the declining phase of a solar cycle. In some cases, coronal holes can last for several solar rotations (for several months).

Magnetic fields flowing out of coronal holes are open, expanding into interplanetary space without returning to the Sun. These unipolar magnetic fields accelerate the solar wind flowing out of a coronal hole forming what is known as high-speed stream (HSS). In fact, long-lasting coronal holes are a major source of high-speed streams that can buffet Earth for many days and then reoccur every 27 days as the Sun rotates. Like the coronal holes from which they flow, high speed streams occur most frequently during the declining phase of the solar cycle.

20.1.5 Solar Winds

Solar winds consist of hot plasma (electrons and positively charged ions) that continuously flow outward at various speeds from coronal holes, CMEs, solar flares, and other disturbances on the Sun.

Solar winds deform Earth's magnetic field into a comet shaped magnetosphere illustrated in Figure 8. The bow shock always faces toward the Sun while the magnetosphere tail faces away from the Sun, the same as comets. The Earth rotates within the stationary magnetosphere.

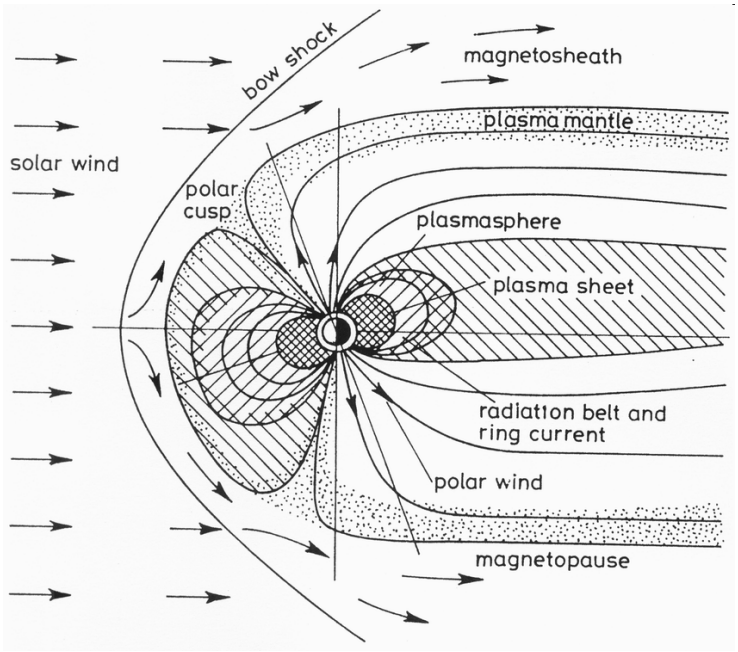

Figure 8 Earth's magnetosphere (source: Davies)

Slow speed background solar wind emanates from the Sun all the time. Higher speed winds are produced by coronal holes, CMEs, and solar flares. The solar wind is very tenuous with a density around 5 particles per cm^3. In contrast, the electron density of the F region ionosphere is around a million particles per cm^3. Wind speeds range from about 250 to 750 km/s near Earth. Again, 447 km/s is equal to 1 million per hour. Solar wind temperature near Earth is 100,000 to 150,000 ^oK.

An extremely important characteristic of the solar wind is that it contains an embedded magnetic field. The magnetic field is known as the Interplanetary Magnetic Field (IMF). The magnetic field originates internal to the Sun. However, in the corona a small portion of the Sun's magnetic field becomes "frozen in" the solar wind plasma due to the plasma's very high electrical conductivity.

The IMF propagates throughout the solar system, carried along by the solar wind, hence its name "interplanetary magnetic field". The strength of the IMF field averages only about 5.6 nT. In comparison, the strength of Earth's geomagnetic field is between 25,000 to 65,000 nT at Earth's surface. Earth's magnetic field drops to 0 nT at the outer edge of the magnetosphere where it comes in contact with the IMF. The direction of the IMF relative to Earth's magnetic field is constantly changing. A southward directed IMF points in the opposite direction of Earth's magnetic field. A southward IMF arriving at Earth will couple with Earth's northward magnetic field generally producing an ionospheric storm. Very few storms if any occur when the IMF arriving at Earth is pointed northward.

20.2 Ionospheric Storms

As indicated above, there are three types of ionospheric storms:

- X-ray radiation storms,
- High energy particle storms, and
- Solar wind storms.

These are each described in the following sections.

20.2.1 X-ray Radiation Storms

An x-ray radiation storm is produced by a sudden intense increase in x-ray radiation from the Sun following a solar flare. Radiation from a flare reaches Earth in a little over 8 minutes. The resulting radiation storm dramatically increases D layer absorption in daylight regions of the Earth, usually blacking out HF radio communications in the area.

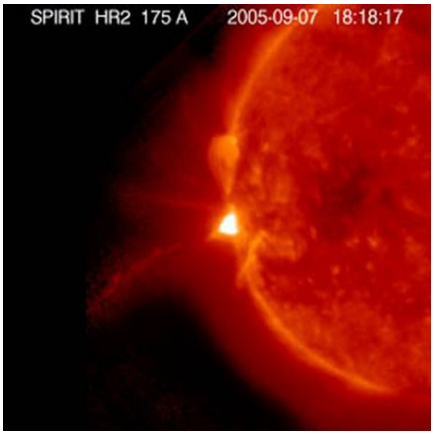

Figure 9 Image of the solar flare occurring on September 7, 2005 taken by the Soviet Union Spirit spacecraft.

The x-ray radiation from the solar flare shown in Figure 9 was measured by a GOES satellite (Figure 10) in synchronous orbit around the Earth. Note that x-ray radiation cannot be detected by ground level sensors since solar x-ray radiation is completely absorbed in the ionosphere.

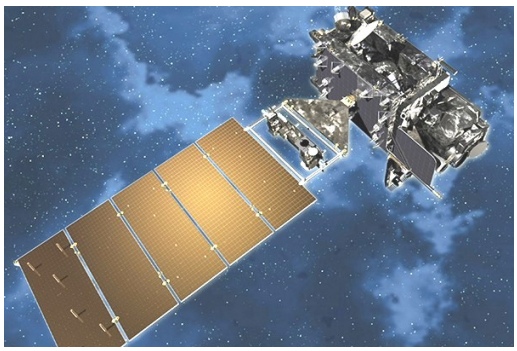

Figure 10 GOES Spacecraft (Source: NOAA)

This was a particularly large solar flare. The red trace in Figure 11 shows that the x-ray flux measured by the GOES satellite increased a thousand times in a little under ten minutes. The vertical axis in Figure 11 indicates the strength of the x-ray radiation. The axis is similar to the earthquake Richter scale. Each band (A, B, C, etc.) represents a times 10 increase in x-ray radiation strength.

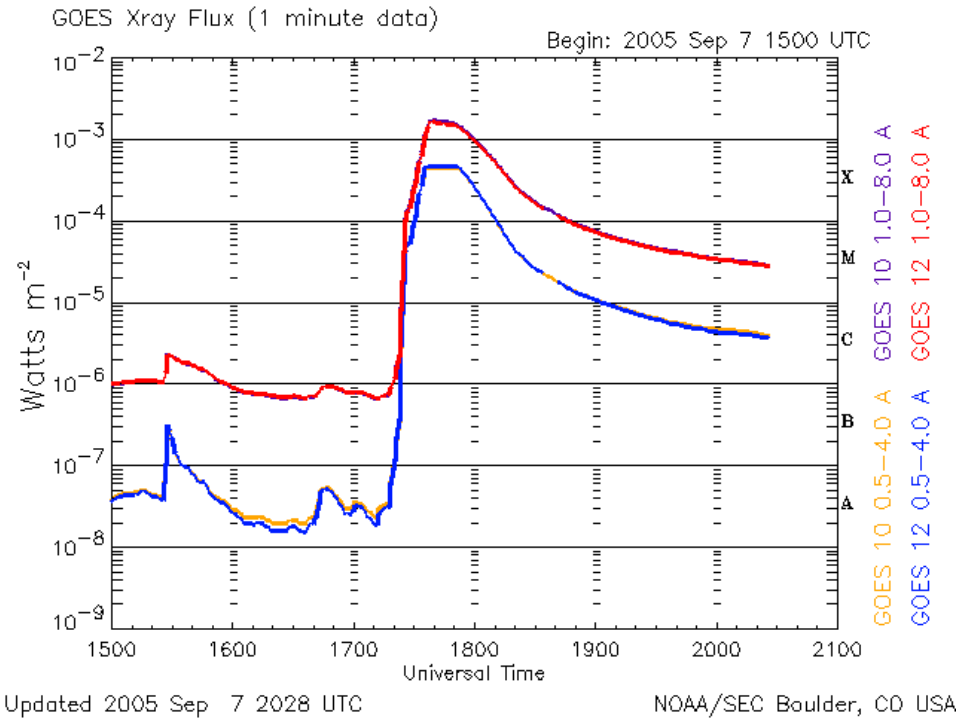

Figure 11 X-ray Flux for September 7, 2005 solar flare (source NOAA)

An x-ray radiation storm is large impacting all latitudes with the greatest impact at local noon in the tropics where the Sun is directly overhead. Figure 12 shows the extent of the large x-ray radiation storm occurring on September 7, 2005. This particular storm heavily ionized the D layer causing extensive absorption of HF radio signals throughout North and South America. The black diamond in Figure 12 represents the Sun's position at local noon. In this figure the Sun was located above the Pacific Ocean south of Central America. The colored bands indicate the highest radio frequencies affected by the flare. In this case, all frequencies below 25 MHz were affected throughout North and South America, pretty much blacking out all HF radio communications in the region. The bar graph on right side of the figure shows signal attenuation by frequency, with lowest frequency signals attenuated the most.

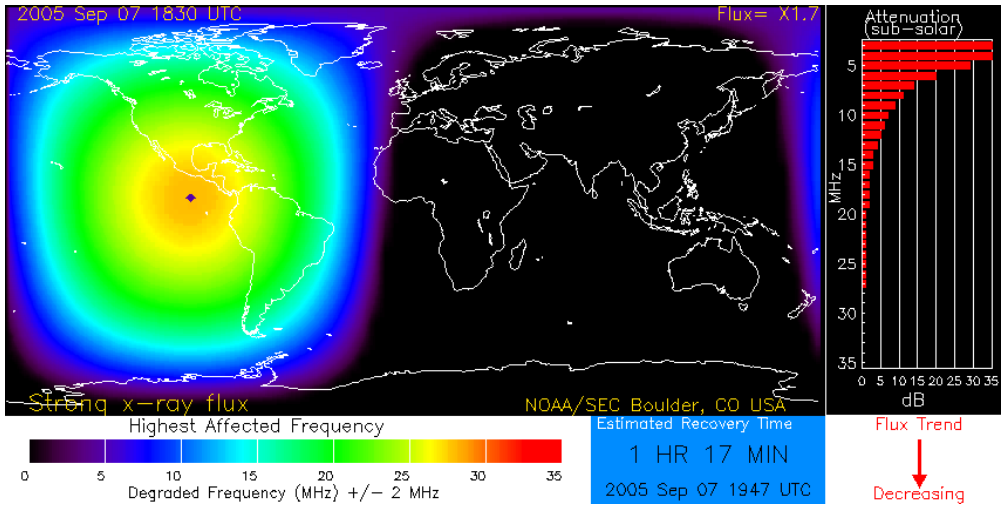

Figure 12 Radio signal absorption during September 7, 2005 solar flare (source: NOAA)

At the time this flare occurred several amateur radio operators, including the author, had just concluded participation in a weekly 40-meter California emergency communications net. Prior to the net we checked propagation conditions by monitoring the National Institute of Standards and Technology (NIST) WWV radio station transmitting on 5, 10, 15, and 20 MHz. Strong signals were received on all 4 frequencies. The emergency net went well with stations throughout California being easily received. Following the net we check WWV again. To our surprise, 5 MHz was completely dead. 10 MHz was shaky with rapid fading in and out. 15 and 20 MHz were both solid. We tuned back down the bands. 15, 10, and 5 MHz were now completely dead. We tuned back up to 20 MHz and found that it was dead also. This sequence of events is typical for the onset of a major x-ray radiation storm. The lowest frequency signals are lost first with progressively higher frequency signals lost in order.

An x-ray storm can last from a few minutes to several hours. This particular x-ray storm lasted a considerable part of the day. The region of the Earth affected by an x-ray radiation storm moves westward as the Earth rotates to the east. This x-ray storm impacted the far east (Korea, Japan, China, etc.) later in the day.

If an x-ray storm occurs in the morning local time, as it did in Figure 9 for Japan, the best long distance radio communications is with stations to the west, away from the approaching storm. If it occurs in the afternoon local time, as it did for Europe, the best communications is to the east, again away from the storm. If the storm hits around noon there is nothing you can do about it. Go have a good lunch. However, later in the afternoon look to the east for radio signal recovery as the storm moves westward.

20.2.2 High Energy Particle Storms

High energy particle storms are produced by solar energetic particles (SEPs) bombarding the Earth following a massive eruption on the Sun. These eruptions include the violent collapse of coronal loops, solar flares and CMEs. The energetic particles are primarily protons from hydrogen atoms that have been stripped of their electrons by the intense heat of an eruption. The eruption accelerates the protons to nearly the speed of light causing them to reach Earth in 20 minutes to an hour.

GOES satellites continuously monitor the proton flux arriving from the Sun. The proton flux level is generally quite low as illustrated in Figure 13. The NOAA Space Weather Prediction Center (SWPC) issues a warning if the proton flux energy level exceeds 10 MeV. Proton flux above this level can cause serious problems, including damaging spacecraft, altering the accuracy of GPS navigational systems, and causing biological DNA damage to passengers and crew in aircraft flying over the poles. Airlines must avoid transpolar routes during a high energy particle storm. An electron volt (eV) is the energy acquired by an electron falling through a potential of 1 volt.

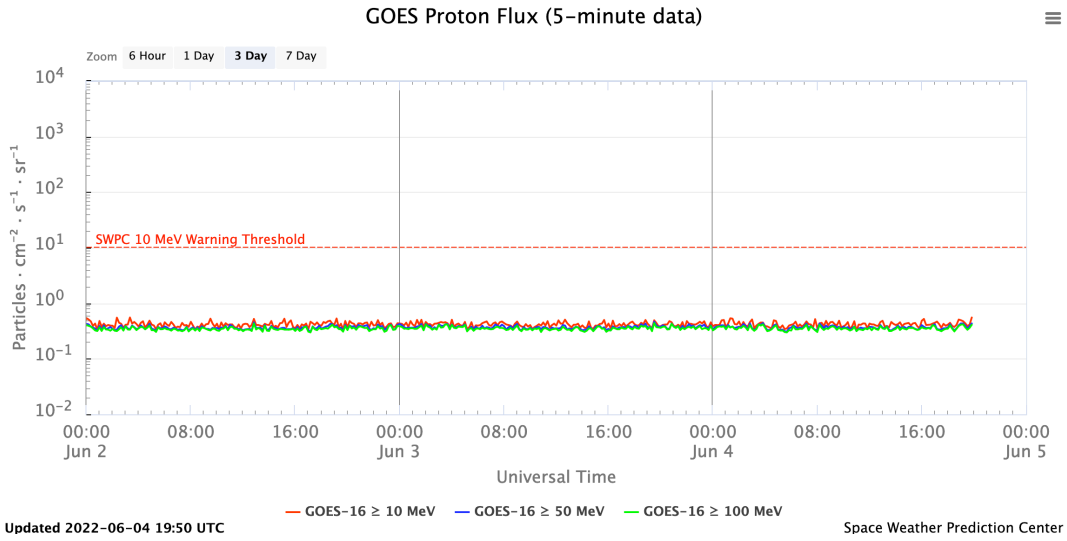

Figure 13 GOES Proton Flux data (source: Space Weather Prediction Center)

The electrically charged energetic particles cannot cross Earth's magnetic field lines. Instead, they are forced to travel along the magnetic field lines, as illustrated in Figure 14. The particles spiral down the magnetic field lines into the Earth's polar regions heavily ionizing the polar ionosphere's D region.

The extensive ionization causes HF radio signals passing through the area to be heavily absorbed. This is known as a Polar Cap Absorption event (PCA). Lower frequency signals are more heavily absorbed than higher frequencies, as is the case in all D-layer absorption phenomena. In extreme cases, a complete radio blackout can occur over the poles lasting for several days. It is important to note that a PCA is a consequence of a storm. As noted earlier, other consequences include damage to spacecraft, errors in GPS systems, and rerouting of transpolar airline routes.

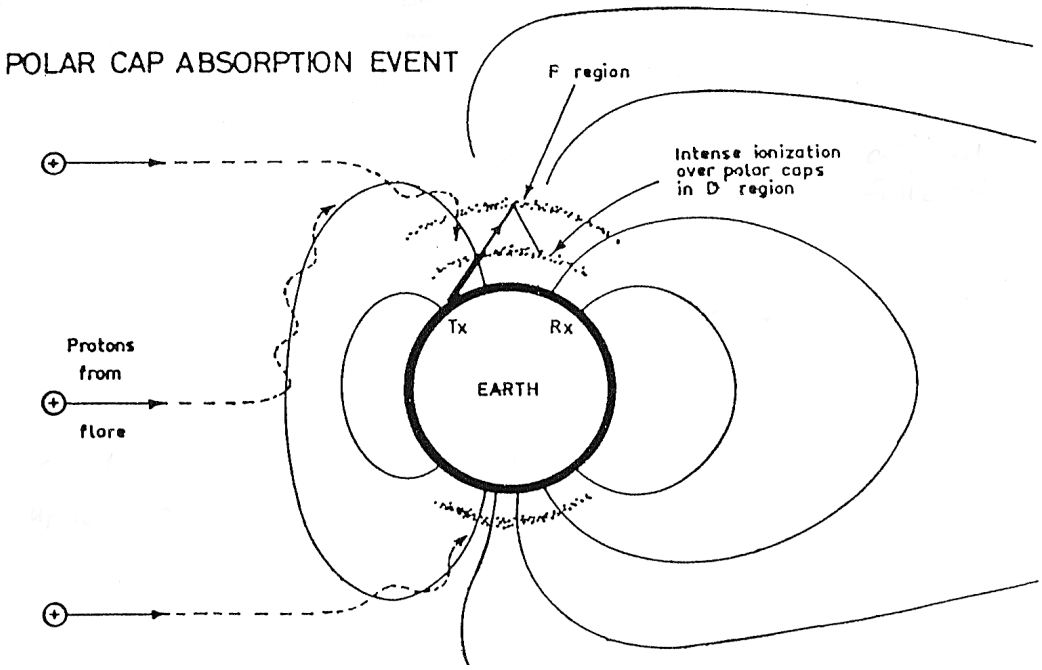

Figure 14 Polar Cap Absorption event (source: McNamara)

High energy particle storms occur more often during solar maximum when solar flares and CMEs are prevalent. It is not unusual for polar cap absorption events to occur in groups with two or more PCAs occurring within a few days of each other. PCAs also tend to occur more during daylight hours than at night. This is to be expected. SEPs from a solar eruption reach Earth in 20 minutes to an hour. Thus, it is the Sun lit part of the Earth that will be blasted by the solar energetic particles. A PCA first appears at very high latitudes and then expands toward the equatorial edge of the polar cap.

Only the largest eruptions on the Sun emit charged particles with high enough energy to produce PCAs. To ionize the polar D layer, SEPs must have enough energy to penetrate through the F and E

regions with sufficient energy left to ionize D-layer molecules. Solar energetic particles must have energy levels greater than 20 MeV to do this. Consequently, polar cap absorption events occur infrequently, typically around 10 per year during solar maximum and only one or two per year during solar minimum.

On February 12 and 13, 2024 the proton flux level (red trace in Figure 15) considerably exceeded the SWPC 10 MeV Warning Threshold. The high flux level triggered Polar Cap Absorption events in both the northern and southern polar regions. The PCAs resulted in very high absorption levels throughout the polar regions (the red areas in Figure 16). The southern polar cap PCA was actually more wide spread than the one occurring in the northern polar cap region. Again, this is to be expected. February was summer in the southern hemisphere with the southern polar region in Sun light most of the time.

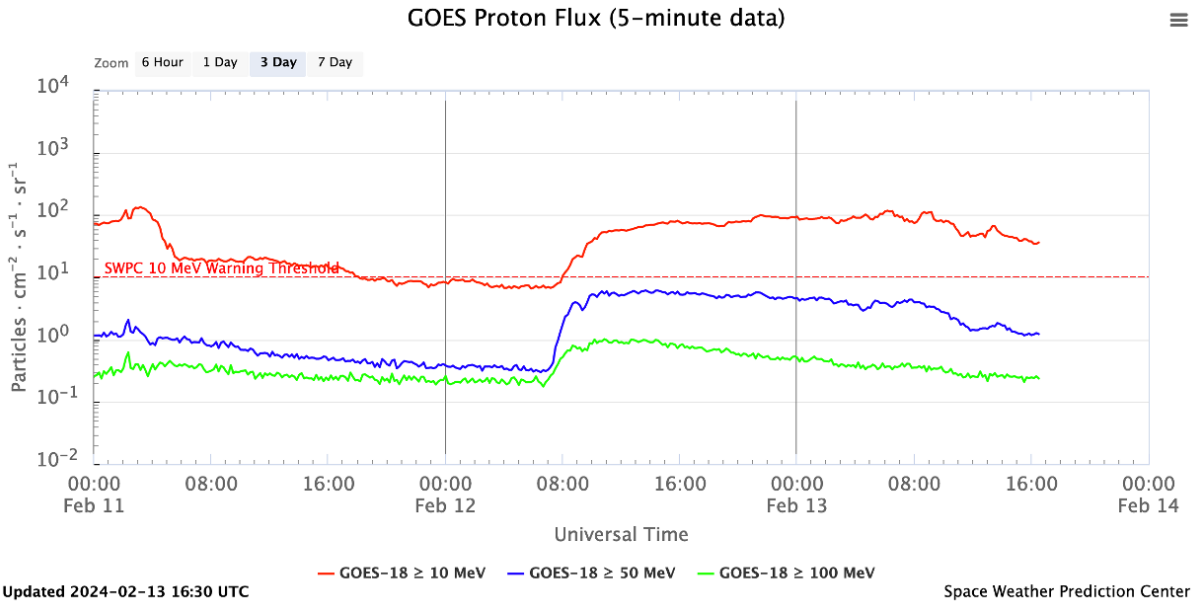

Figure 15 Proton Flux data for February 11 through 13, 2024 (source: SWPC)

It is worth noting that high energy particle storms also ionize polar cap atoms and molecules in the F and E regions. This ionization increases F and E region electron densities which is conducive to HF radio wave propagation. But this beneficial ionization is masked by intense D layer absorption.

Current proton flux data is available by clicking on “Proton Flux” under the “Current Conditions” tab of the www.skywave-radio.org website.

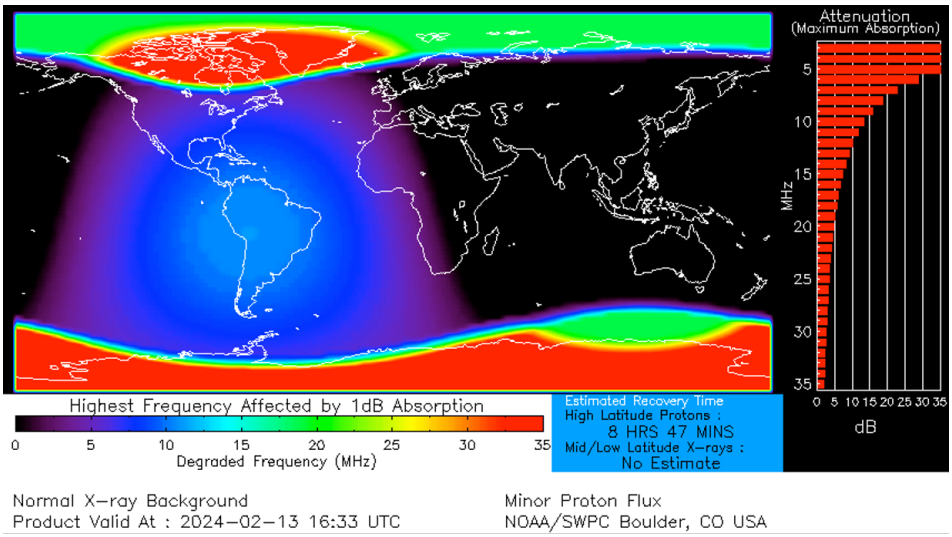

Figure 16 Polar Cap Absorption event occurring on 2/13/2024 (source: NOAA/SWPC

20.2.3 Ionospheric Solar Wind Storms

Ionospheric solar wind and geomagnetic storms are quite different, even though they both originate from the same solar wind phenomena. Both types of storms are caused by strong solar winds with southward directed interplanetary magnetic fields (IMF). Geomagnetic storms cause significant dips and fluctuations in Earth's magnetic field. In contrast, ionospheric storms are characterized by large drops in F2 critical frequencies. Ionospheric solar wind storms typically originate in the auroral ionosphere and drift into the mid-latitudes, carried along by thermospheric winds.

20.2.3.1 Solar Wind High Speed Streams (HSS)

Collapsing coronal loops, solar flares, CMEs, and coronal holes eject billions of tons of coronal material into interplanetary space. The ejected material forms solar wind high speed streams (HSS) that travel in rotating spirals outward from the Sun as illustrated in Figure 17. Embedded in the ejected material is the weak Interplanetary Magnetic Field (IMF) which has a significant impact on ionospheric storms. The speed of the HSS winds is considerably higher than the steady background solar wind.

The solar wind actually flows out radially from the Sun. However, the Sun's rotation causes the high-speed streams to take on their spiral shape when viewed from above. X-ray radiation and high energy protons also follow spiral paths to Earth, but their transit time is so short relative to the Sun's rotation that the spiral shape is not apparent.

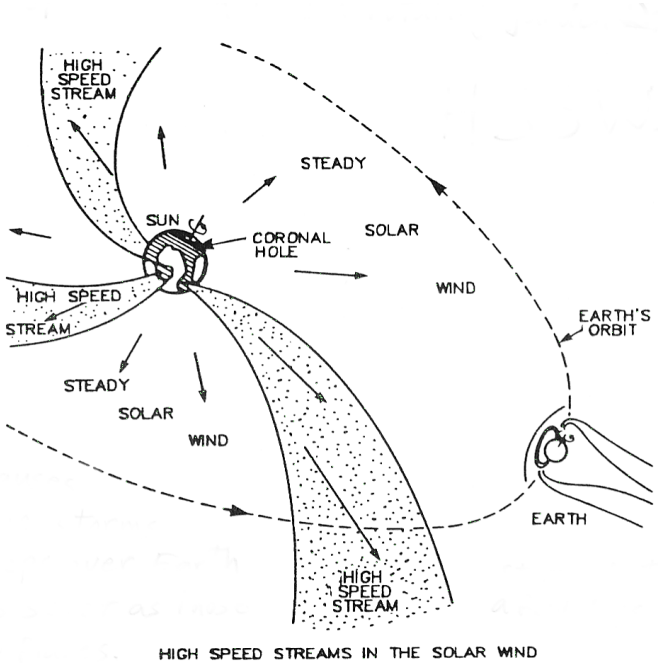

Figure 17 Solar Wind High Speed Streams (source: McNamara)

The HSS wind and its embedded IMF field reach Earth in about two to four days. When the wind arrives one of two things can happen. If the continuously rotating IMF happens to be directed northward, very little if anything happens. However, if the IMF is pointed southward, it connects to Earth's northward magnetic field. The interconnected magnetic fields are dragged across the polar region by the solar wind. In the process, the polar region magnetic field lines are pealed open in the vicinity of the polar cusp allowing charged solar wind particles to stream down into the magnetosphere. In Figure 18 the polar cusp is located just inside the magnetosphere's bow shock. The polar cusp forms the gap between the day side magnetic field extending out in front of the Earth and the nightside field forming the magnetotail. There are two polar cusps, one in the northern polar region and a second one in the southern polar region.

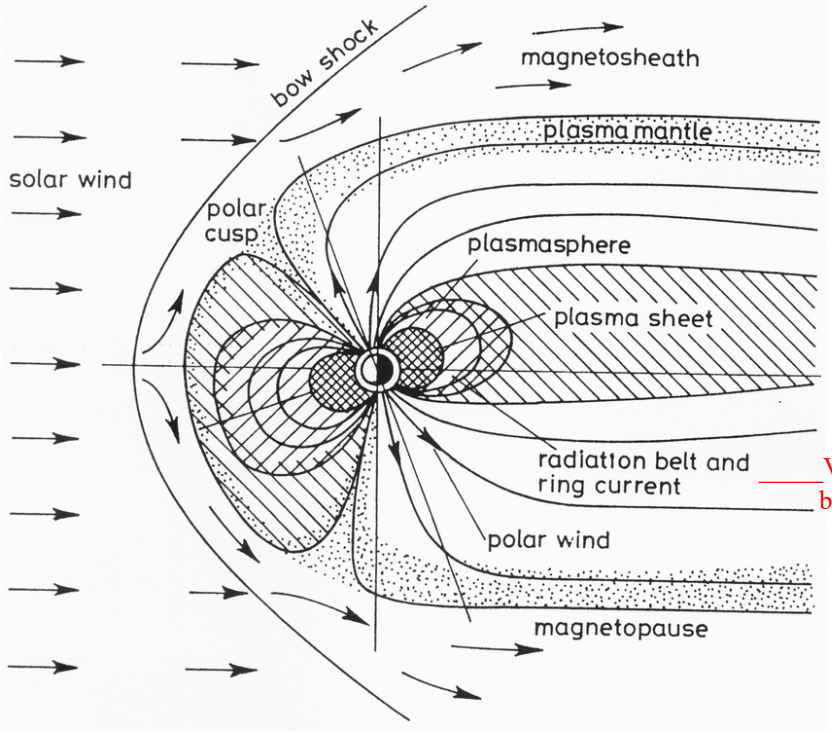

Figure 18 Earth's Magnetosphere (source: Davies)

Some of the particles streaming into the magnetosphere become trapped in Earth's two donut shaped Van Allen radiation belts. The radiation belts are located in the magnetosphere relatively close to the Earth as shown in Figure 18. The outer radiation belt (Figure 19) stretches from 12,000 out to 25,000 miles above the Earth. The inner belt is much closer occupying the area from 1,000 to 8,000 miles from the Earth. Most spacecraft with long duration missions, including commercial, scientific, and military spacecraft, are positioned in geosynchronous orbit 22,000 miles over Earth's equator. These spacecraft, represented in Figure 19 by NASA's Solar Dynamic Observatory, orbit in the outer belt close to the belt's upper boundary. The constellation of global positioning satellites (GPS) orbit at the lower edge of the outer belt. Satellites in low earth orbit (LEOs), including the International Space Station orbiting at 230 miles, orbit in a region below the inner belt.

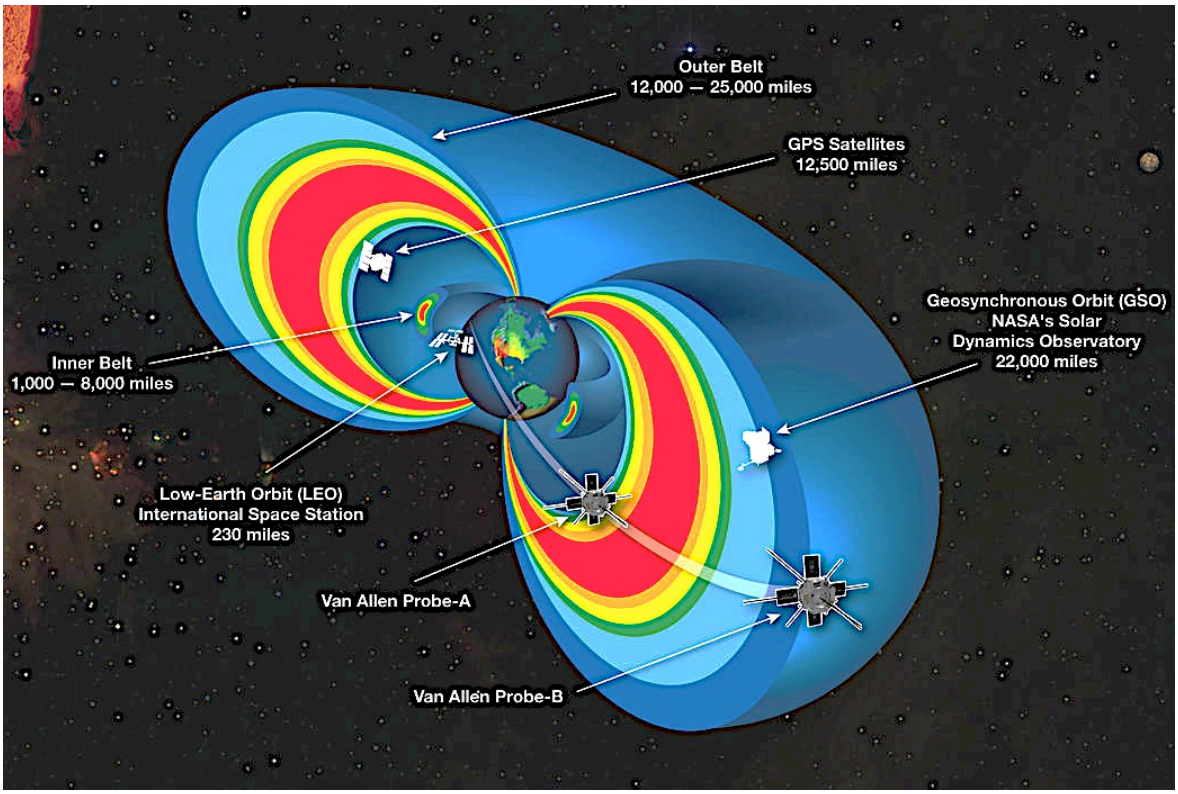

Figure 19 Cutaway model of the radiation belts (source: NASA)

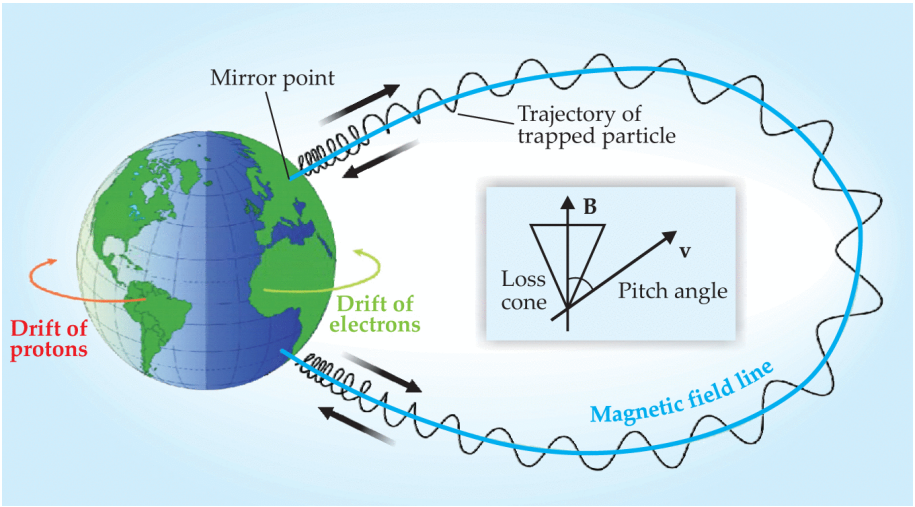

Figure 20 Trapped Charged Particles (source: Physics Today – Scitation)

The particles trapped in the Van Allen belts bounce back and forth along magnetic field lines between Earth's north and south polar regions as illustrated in Figure 20.

20.2.3.2 Equatorial Ring Current

At an altitude of approximately 10,000 miles (16,000 km) above the equator gradients in Earth's magnetic field cause the trapped positively charged particles to drift westward while the trapped electrons drift to the east, creating a westward equatorial ring current. In Figure 20 the positively charged particles drifting westward are shown in red while the electrons drifting eastward are shown in green. The ring current is positioned between the inner and outer radiation belts.

The equatorial ring current is the primary cause of geomagnetic storms. Normally the ring current is in a quiescent state. However, the strength of the ring current dramatically increases when a HSS wind sweeps past Earth injecting huge quantities of solar wind particles into the radiation belts.

The ring current produces its own magnetic field. This field opposes that of the Earth creating fluctuations in Earth's magnetic field strength. We define these fluctuations as a geomagnetic storm. The strength of Earth's core field in the equatorial region is around 40,000 nT. In comparison, the strength of the ring current magnetic field is on the order of 200 nT during a strong geomagnetic storm. The strength of the ring current field is only one half a percent of the core field. However, the fluctuations that it causes in the core field can potentially cause trillions of dollars in damage to our technological infrastructure, including electrical power outages lasting weeks if not months. For this reason, fleets of spacecraft are in orbit around the Earth and Sun continuously monitoring solar activity. These spacecraft provides us with an early warning system of impending geomagnetic storms, providing us with time to put critical systems into a "safe mode".

20.2.3.3 Development of Ionospheric Solar Wind Storms

Development of an ionospheric solar wind storm is much different.

Not all of the solar wind particles streaming down into the magnetosphere are captured in the radiation belts. Some continue down through the radiation belts into Earth's auroral zone as illustrated in Figure 21.

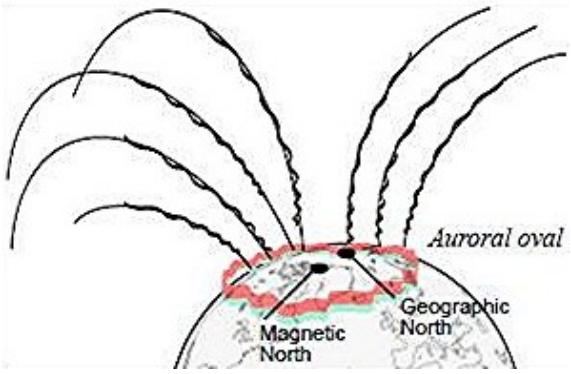

Figure 21 Particles flowing into Auroral Oval (source: NOAA Space Environment Center)

Collisions of these particles with neutral atoms and molecules change the chemical composition of the auroral ionosphere, heat the atmosphere, and change the circulation patterns of thermospheric wind. Heating plus changes in chemical composition accelerates the recombination of electrons with ions, decreasing electron densities in the auroral ionosphere.

Convection currents carry the electron depleted auroral plasma down into mid latitudes causing F2 layer critical frequencies to drop by a factor of 2 or more. The drop in critical frequency impacts the higher HF bands more than lower frequencies. Radio frequencies from 20 through 10 meters are affected the most. These bands often disappear for a week or more.

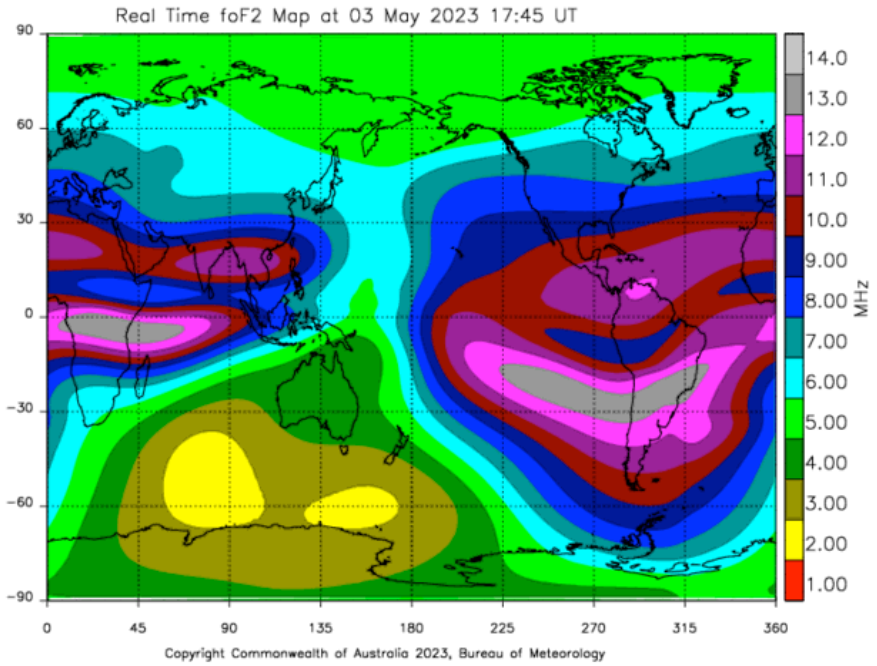

Figure 22 Critical frequency map in the absence of a solar wind storm

Figure 22 shows a typical critical frequency map in the absence of a solar wind storm. Notice in this figure that critical frequencies over the United States range from 7 MHz in the northern states to 10 MHz over Miami, Florida. Figure 23 shows the critical frequencies at the same time of day nine days earlier during a solar wind storm. The critical frequencies during the storm were 3 MHz less, nearly 1/2 the critical frequencies for non-storm conditions.

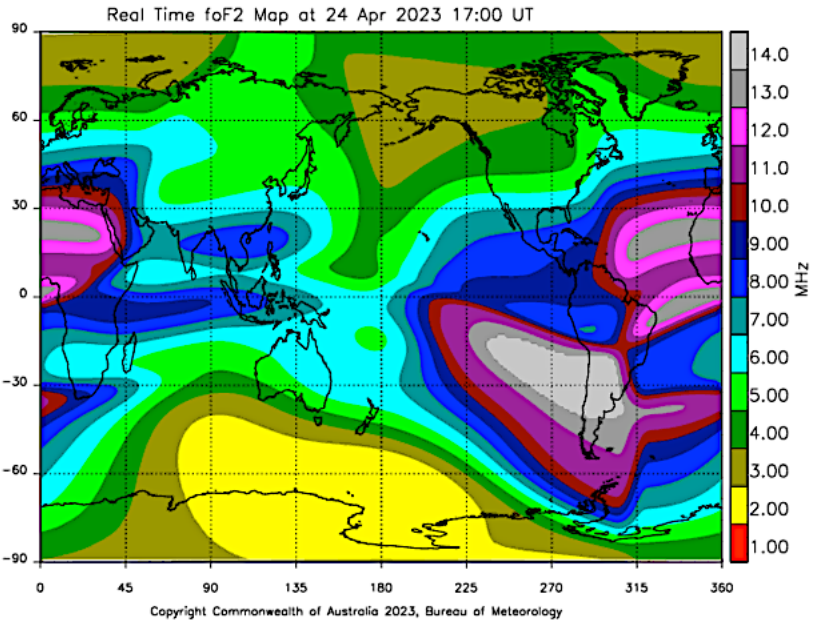

Figure 23 Critical frequency map during a solar wind storm

20.2.3.4 Highest Occurrence of Solar Wind Storms

Surprisingly, the highest occurrence of solar wind storms is during the declining phase of the solar cycle, one to two years following solar maximum as illustrated in Figure 24. These storms are produced primarily by coronal holes. In Figure 24, the number of sunspots is shown by the red trace while the number of disturbed days caused by ionospheric solar wind and geomagnetic storms is shown by the blue trace.

Unlike solar flares, coronal hole induced solar wind storms are not preceded by x-ray and high energy particle storms. Coronal hole solar wind storms are most likely to occur in the spring and fall during the declining phase of a solar cycle. In the spring and fall Earth's magnetic field is favorably aligned with the IMF increasing the chance of intense geomagnetic and ionospheric storms. Coronal hole induced storms also occur during the active phase of the solar cycle but are less in number than solar flare and CME induced storms.

Coronal holes can last for a long time. Consequently, as illustrated in Figure 25, the high-speed solar wind flowing out of a particular coronal hole can sweep past Earth with each solar rotation causing ionospheric solar wind storms that reoccur every 27 days.

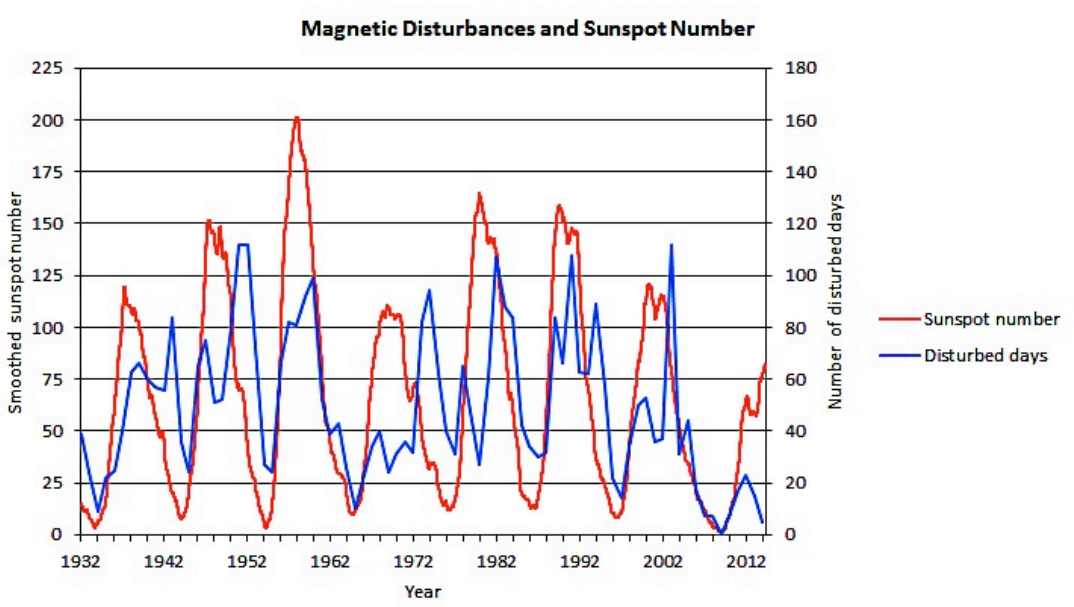

Figure 24 Occurrence of solar wind storms (source: Space Weather Services)

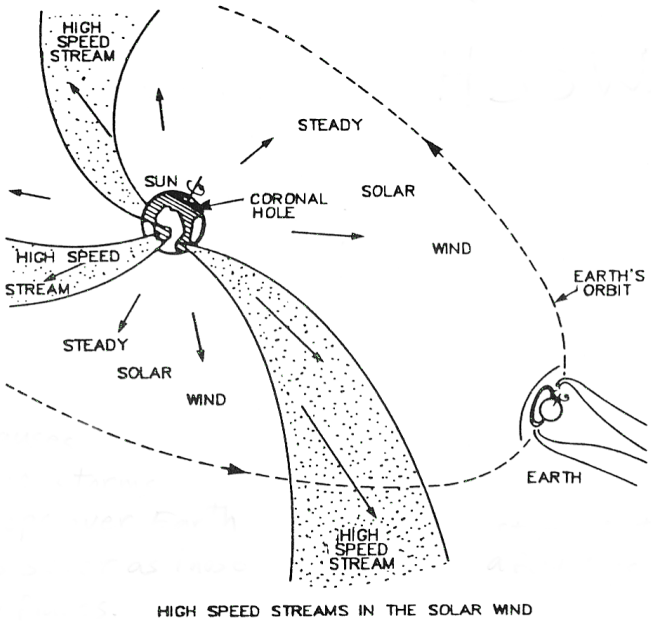

Figure 25 Solar Wind High Speed Stream (source: McNamara)

20.2.3.5 Planetary K Index

Figure 26 shows the planetary K – index for September 27 through 30, 2020. The planetary K – index is a measure of geomagnetic activity. A low K_p value ($K_p < 4$) indicates that Earth's magnetic field is quiet, solar winds are subdued, and the equatorial ring current is in a quiescent state. A K_p value around 4 indicates that the magnetic field is moderately disturbed as the result of a modest solar wind and some enhancement of the equatorial ring current. A high K_p value, greater than 4, signifies that a strong solar wind with a southward directed IMF is impacting Earth's magnetosphere, greatly enhancing the ring current and producing an intense geomagnetic storm. The characteristics of the storm include rapid fluctuations in Earth's magnetic field along with field strengths below their nominal level.

The K_p value is obtained by averaging together the amplitude and phase of the magnetic field measured over a 3-hour period. The measurements are performed at 12 magnetic field observatories around the world. The observations from the various observatories are combined together to provide the planetary K_p value. The value of K_p for each 3-hour period ranges from 0 (very quiet) to 9 (very disturbed) on a quasi-logarithmic scale. Notice in Figure 26 that green bars ($K_p < 4$) indicate quiet geomagnetic conditions. Yellow bars ($K_p = 4$) signify minor storms and red bars ($K_p > 4$) indicate major to severe storms.

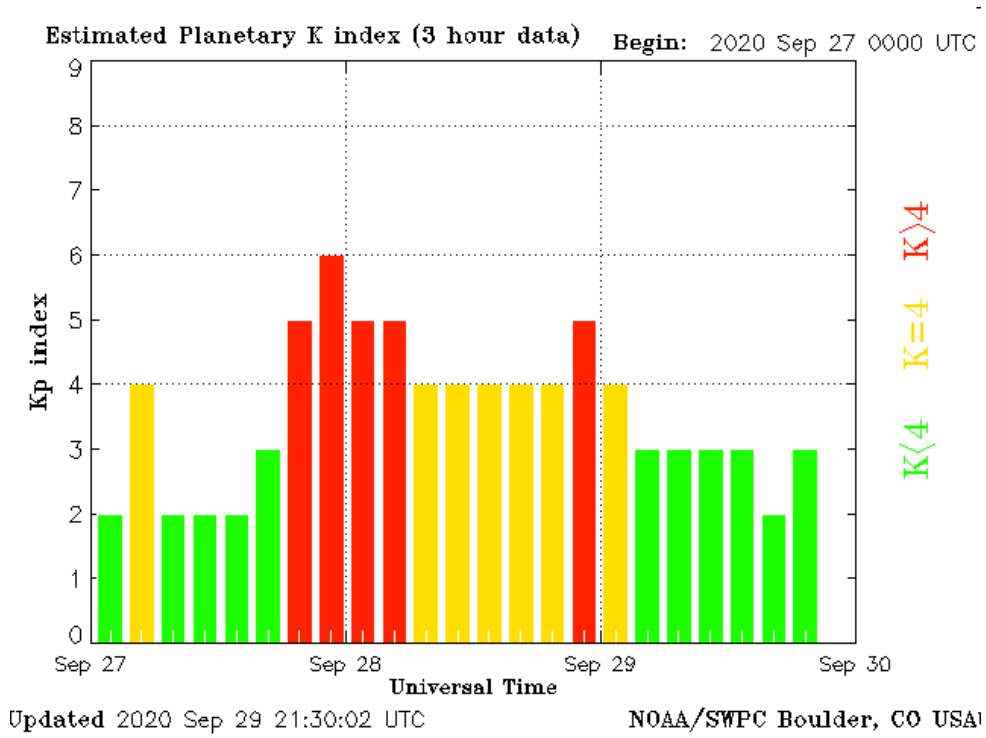

Figure 26 K_p Values for September 27 – 30, 2020

While the K_p value is a measure of magnetic field activity, it also provides a reasonably good indication of ionospheric solar wind storms since geomagnetic and ionospheric storms are produced by the same solar wind phenomena. A high K_p value indicates that an ionospheric solar wind storm is probably occurring at polar and mid-latitudes, suppressing F2 critical frequencies, and adversely affecting radio operations on 20 through 10 meters.

The current K_p index value can be obtained by clicking on "K_p Index" under the "Current Conditions" tab at www.skywave-radio.org.

References

Hunsucker R. D.; Hargreaves, J. K.; "The High-Latitude Ionosphere and its Effects on Radio Propagation"; Cambridge University Press 2003

Davies, Kenneth; "Ionospheric Radio"; Peter Peregrinus Ltd.,1990

McNamara, Leo F.; "The Ionosphere: Communications, Surveillance, and Direction Finding"; Krieger Publishing Company, 1991

Bridgman, Tom; "PlasmaZoo: E-cross-B Drift"; NASA Visualizations, https://svs.gsfc.nasa.gov/4265 ; February 2, 2015

Casey, John P; "Overview of the Equatorial Electrojet and Related Ionospheric Current Systems"; NUWC-NPT Technical Report 11, 676 25 April 2005

Pitkanen, Timo; "Dynamics Of The Polar Cap Boundary And The Auroral Oval In The Nightside Ionosphere"; Department of Physics University of Oulu, Finland, June 2011

Nichols, Eric P.; "Propagation and Radio Science"; The American Radio Relay League, Inc. 2015

Yeang, Chen-Pang; "Probing The Sky With Radio Waves"; The University of Chicago Press, 2013

Devoldere, John; "Low-Band DXing" fourth edition; ARRL, 2005

Levis, Curt A. ; Johnson, Joel T.; and Teixeira, Fernando L.; "Radiowave Propagation Physics and Applications"; John Wiley & Sons, Inc., 2010

Ahrens, C. Donald; "Essentials of Meteorology"; Wadsworth Publishing Company, 1998

UCAR Center for Science Education (UCAR SciEd); https://scied.ucar.edu/learning-zone/atmosphere/

Khazanov, George V.; "Space Weather Fundamentals"; CRC Press, 2016

Foukal, Peter; "Solar Astrophysics third edition"; Whiley-VCH Publishing Company, 2013

Ganushkina, N. Yu.; Liemohn, M. W.; Dubyagin. S.; "Current Systems in the Earth's Magnetosphere"; AGU, March 8, 2018

Gallagher, Dr. D.L.; "The Earth's Plasmasphere"; Space Plasma Physics, Marshall Space Flight Center, Huntsville, Al, September 05, 2018

Moore, T. E., Morwitz, J. L.; "Stellar Ablation of Planetary Atmospheres"; August 9, 2007

Yau, Andrew W.; Abe, Takumi; Peterson, W. K.; “The Polar Wind: recent Observations”; Department of Physics and Astronomy, University of Calgary

Carroll, Bradley W. and Ostlie, Dale A.; “An Introduction to Modern Astrophysics”; Addison-Wesley Publishing Company Inc., 1996

Goodman, John M.; “Space Weather & Telecommunications”; Springer Science+Business Media Inc. 2005

Cander, Ljiljana R.; “Ionospheric Space Weather”; Springer Nature Switzerland AG 2019

Moldwin, Mark; “An Introduction to Space Weather”; Cambridge University Press, 2008

Campbell, Wallace H.; “Introduction to Geomagnetic Fields”; Cambridge University Press, 2003

Golub, Leon and Pasachoff, Jay M.; “Nearest Star The Surprising Science of Our Sun second edition”; Cambridge University Press, 2014

Loff, Sarah: ”Explorer and Early Satellites”; National Aeronautics and Space Administration, Aug 3, 2017

Minzner, R. A.; “The 1976 Standard Atmosphere Above 86 km Altitude” NASA Goddard Space Flight Center, 1976